The Change of Functional Connectivity Specificity in Rats Under Various Anesthesia Levels and its Neural Origin

Xiao Liu,
Department of Radiology, Center for Magnetic Resonance Research, University of Minnesota, 2021 6th St. SE, Minneapoli, MN 55455, USA

Department of Biomedical Engineering, University of Minnesota, 2021 6th St. SE, Minneapoli, MN 55455, USA

Xiao-Hong Zhu,
Department of Radiology, Center for Magnetic Resonance Research, University of Minnesota, 2021 6th St. SE, Minneapoli, MN 55455, USA

Yi Zhang, and
Department of Radiology, Center for Magnetic Resonance Research, University of Minnesota, 2021 6th St. SE, Minneapoli, MN 55455, USA

Wei Chen
Department of Radiology, Center for Magnetic Resonance Research, University of Minnesota, 2021 6th St. SE, Minneapoli, MN 55455, USA

Department of Biomedical Engineering, University of Minnesota, 2021 6th St. SE, Minneapoli, MN 55455, USA

Wei Chen: wei@cmrr.umn.edu

Abstract

Spatiotemporal correlations of spontaneous blood oxygenation level dependent (BOLD) signals measured in the resting brain have been found to imply many resting-state coherent networks under both awake/conscious and anesthetized/unconscious conditions. To understand the resting-state brain networks in the unconscious state, spontaneous BOLD signals from the rat sensorimotor cortex were studied across a wide range of anesthesia levels induced by isoflurane. Distinct resting-state networks covering functionally specific sub-regions of the sensorimotor system were observed under light anesthesia with 1.0 % isoflurane; however, they gradually merged into a highly synchronized and spatially less-specific network under deep anesthesia with 1.8 % isoflurane. The EEG power correlations recorded using three electrodes from a separate group of rats showed similar dependency on anesthesia depth, suggesting the neural origin of the change in functional connectivity specificity. The specific-to-less-specific transition of resting-state networks may reflect a functional reorganization of the brain at different anesthesia levels or brain states.

Keywords

Functional MRI (fMRI); BOLD; Resting-state fMRI (rs-fMRI); Functional connectivity; Anesthesia; Animal models; Neural origin

Correspondence to: Wei Chen, wei@cmrr.umn.edu.

Introduction

Many resting-state functional magnetic resonance imaging (rs-fMRI) studies have shown that the blood oxygenation level dependent (BOLD) signals recorded from the resting brain are characterized by spontaneous and coherent fluctuations at low frequency within a variety of anatomically-connected and functionally-specific brain networks (Biswal et al. 1995; Fox and Raichle 2007; Zhang and Raichle 2010). It has been suggested that such spontaneous BOLD fluctuations may reflect ongoing brain activity under the resting state and their temporal correlations could reflect the "functional connectivity" (Biswal et al. 1995) and imply many "resting-state brain networks" (Mantini et al. 2007). These findings are of great importance, because they may potentially explain the large portion of biochemical energy "mysteriously" consumed by the resting brain for supporting spontaneous neuronal activity (Raichle 2006; Shulman et al. 2007; Du et al. 2008), and provide new insights into fundamental mechanisms of brain function and network.

Rather than the fluctuations of unconstrained and consciously directed mental activity, the spontaneous BOLD fluctuations and associated resting-state coherent networks are believed to reflect a more fundamental and intrinsic organization of the resting brain. They have been widely observed not only in awake human brains but also under brain states with a reduced level or complete loss of consciousness, for example, during sleep, under light sedation, deep anesthesia, or even in the vegetative state (Boly et al. 2009; Greicius et al. 2008; Horovitz et al. 2008; Lu et al. 2007; Vincent et al. 2007). A recent rat study has shown that even in the deeply-anesthetized, unconscious brain state characterized by burst-suppression (BS) electroencephalogram (EEG) pattern, the spontaneous BOLD correlations still implied a highly coherent but less-specific resting-state network covering a large cortical region associated with sensorimotor and other brain functions, and the BOLD fluctuations tightly correlated to the power fluctuation of the BS EEG signal (Liu et al. 2011). However, the strong and widely distributed correlation of spontaneous BOLD signals under such a deep anesthesia condition is, to some extent, against intuition. Moreover, such a less-specific pattern of the resting-state network is distinct from those observed in the rats anesthetized with different types and doses of anesthetics covering more specific brain regions, e.g., the bilateral primary somatosensory cortex forelimb (S1FL) regions (Lu et al. 2007; Zhao et al. 2008; Williams et al. 2010).

The apparent discrepancy in the spatial specificity of resting-state networks raises several interesting questions: what causes this discrepancy, different types or different levels of anesthesia used by these studies? Moreover, does the specificity difference of functional connectivity reflect the change of underlying neural activity or other non-neuronal factors?

This work aimed to quantitatively study the relationship between the specificity of resting-state BOLD coherent network and the anesthesia depth using a rat model. To minimize the confounding effects potentially caused by different anesthetics, only isoflurane was applied in the present study, and spontaneous BOLD signals were imaged from the rat brain under three isoflurane levels of ~1.0, ~1.5 and ~1.8 % (defined as light, moderate, and deep anesthesia condition, respectively) during the same experimental session. Through the spatiotemporal correlations of acquired BOLD signals, the resting-state coherent networks and their specificity were examined and compared across different anesthesia conditions.

To further investigate the neurophysiological basis of the changes of network specificity imaged by rs-fMRI, the EEG signals were recorded in the somatosensory cortex using three electrodes from another group of rats under the same anesthesia conditions and their power correlations between different brain regions were analyzed and then compared to the rs-fMRI results. The comparison results were used to test the hypotheses that the anesthesia

depth modulates the specificity of resting-state network and this modulation reflects the change of underlying neural activity.

Materials and Methods

Animal Preparation

Two groups of Sprague-Daley rats (242–341 g body weight) were used for this study. One group of eight rats (Rat 1–8; Group I) were used for MRI experiments, while the other group of six rats (Rat 9–14; Group II) were used for EEG experiments. Rats were initially anesthetized with ~2 % isoflurane in a mixture of O_2 and N_2O gases with a 2:3 volume ratio. The femoral artery and vein were catheterized for monitoring physiological parameters and blood gas sampling. A ventilation machine was used to mechanically control the animal respiratory rate and volume. The mean arterial blood pressure (MAP), inspired/ expired O_2, CO_2, N_2O, body temperature and heart rate were continuously monitored and recorded during the experiment. Table 1 summarizes the MAP and heart rate data, only changes of less than 13 % were observed across different anesthesia conditions. Arterial blood gas was sampled and measured every 1–2 h. The pO_2, pCO_2, pH and plasma glucose level were maintained within normal physiological limits.

After the study was done, the rats were sacrificed by a bolus injection of KCl solution. All animal experiments were conducted under the protocol approved by the University of Minnesota Institutional Animal Care and Use Committee.

MRI Experiments

All experiments were performed on a 9.4T horizontal magnet (Magnet Scientific, UK) interfaced with a Varian INOVA console (Varian Inc., Palo Alto, CA) using a proton radio-frequency (RF) surface coil. The rat head position was fixed using a home-built head-holder with a mouth-bar and ear-bars to minimize head motion. At the beginning of the experiment, multi-slice T_1-weighted anatomical images were acquired with axial, sagittal, and coronal orientations to identify the rat somatosensory cortex and select appropriate image slice positions for acquiring rs-fMRI data. Then, five consecutive coronal fMRI slices (field of view = 3.2×3.2 cm^2; repetition time (TR)/echo time (TE) = 612/16.5 ms; 64×64 image matrix size; 1 mm slice thickness) were acquired using the gradient-echo echo-planar image (GE-EPI) sequence to cover the rat somatosensory cortex (−4.3 to 0.7 mm from the bregma), which was identified by comparing the stereotaxic rat brain atlas (Paxinos and Watson 1998) and the acquired anatomical images. All rs-fMRI data were acquired when the rats were in darkness and all monitored physiological parameters were within normal ranges and stable.

For each rat, the rs-fMRI measurements were repeated for 3–4 runs under light (~1.0 % isoflurane), moderate (~1.5 % isoflurane), and deep (~1.8 % isoflurane) anesthesia conditions, respectively, and two additional runs right after the rat was terminated. Each rs-fMRI run consisted of 500 GE-EPI volumes (~306 s). Ten dummy scans were also added before each run to avoid the transient BOLD signal change during the initial data acquisition period. Between different anesthesia conditions, the fMRI data acquisition was started at least 10 min after the isoflurane level measured in the exhaled gas from rats had reached a desired, stable level and physiological parameters were within normal ranges. Muscle relaxant (0.1 mg/ kg pancuronium) was applied before the concentration of isoflurane was reduced to 1.0 % to ensure the stable physiological status of rats and minimize stress under the relatively light anesthesia condition.

EEG Experiments

A reference EEG electrode was inserted into the animal's nose as a ground, while three other electrodes were inserted into the rat brain through three small holes opened in the skull, located at the bilateral S1FL (primary somatosensory cortex, forelimb; 0.2 mm anterior to the bregma and ~3–3.5 mm from the brain midline), and the right S1BF (primary somatosensory cortex, barrel field; 1.8 mm posterior to the bregma and ~5 mm from the brain midline). Compared to the locations of seeding reference regions used for generating the BOLD correlation maps (all located in the same brain slice −1.8 mm from the bregma, see the next section), the locations of electrodes at the S1FL sites were moved ~2 mm anteriorly to have adequate space for manipulators holding the adjacent EEG electrodes. EEG signals were sampled at 1 kHz using commercially available EEG equipment (Grass Telefactor, RI) and filtered with a band-pass (0.1–100 Hz) filter.

Same as the rs-fMRI measurements, the EEG signals were recorded under three anesthesia conditions (1.0, 1.5 and 1.8 % isoflurane) with at least 20 min of recording time for each condition. EEG signals used for correlation analysis were all acquired at least 10 min after the isoflurane level measured in the exhaled gas from the rats had reached the desired level. The muscle relaxant was applied before the isoflurane concentration was switched to light anesthesia level of 1.0 % isoflurane.

Data Analysis

All GE-EPI images were first spatially filtered with a Gaussian kernel (FWHM = ~1 mm) to increase signal to noise ratio (SNR), and then motion correction was performed on all data using the 3D registration tool (3dvolreg) of AFNI (Cox 1996). The first 20 image volumes of each run were discarded to further eliminate the transient BOLD signal change during the initial GE-EPI acquisition period. The BOLD signal time course of each image pixel was normalized by its mean, and then band-pass filtered (0.003–0.5 Hz) to remove the DC component, linear drift, and high-frequency noise.

Three 2-pixel × 2-pixel regions located in the left and right S1FL (−1.8 mm from the bregma and ~2.5–3 mm from the brain midline), and the right S1BF (−1.8 mm from the bregma and ~5 mm from the brain midline) regions were selected as the seeding reference regions on the same image slice. For each rs-fMRI run, the BOLD time courses of all image pixels were then cross-correlated (Pearson's correlation) with those extracted from the seeding reference regions to generate three corresponding correlation coefficient (CC) maps.

A region of interest (ROI) was selected based on the anatomical images to cover cortical regions in the left hemisphere. For each correlation map, the CC values within the defined ROI were projected (by averaging) onto a line orthogonal to the brain midline to obtain a profile, revealing how the correlation to the seeding reference regions changes along this line.

A notch filter was applied to raw EEG signals to further suppress the line noise residues (the EEG system contains an integrated hardware notch filter for the line noise), and the EEG signals were then down-sampled to 200 Hz. The EEG signal time courses were divided to 300-s long segments to match the duration of the rs-fMRI runs. For each rat and under each anesthesia condition, there were 4–6 EEG segments for the final correlation analysis. For each segment, the EEG signal was band-pass filtered into band-limited EEG signals in 6 different frequency ranges: wide (0.1–100 Hz), delta (1–4 Hz), theta (5–8 Hz), alpha (9–12 Hz), beta (13–30 Hz), and gamma (30–100 Hz). The Hilbert transformation was then applied to the band-limited EEG signals to extract their envelope amplitudes, which quantify the power of EEG signals (equivalent to square root of the power). Pearson's correlation

coefficients were then calculated to quantify the EEG power correlation between different electrodes.

A linear mixed model regarding "rat" as a random effect was used to summarize the results from different rats and make statistical inference. The analysis was implemented in R (Team 2008) with the "lme4" package (Bates et al. 2011).

Power spectra of both BOLD signals and EEG powers were estimated with a MATLAB (MathWorks, Natick, MA) toolbox named Chronux using a nonparametric multitaper method (Thomson 1982). Data analysis was mainly performed using MATLAB 7.5.

Global Signal Regression

To examine how the removal of global BOLD signal could affect the correlation analysis (i.e., correlation maps), the same fMRI data was reprocessed using a second strategy, in which the global mean signal (averaged within a large ROI covering the whole brain) was removed by linear regression from the BOLD time courses of all GE-EPI image pixels during the pre-processing stage.

Results

Specificity of Coherent Network Changes as Anesthesia Level Varies

Figure 1a shows BOLD correlation maps and their corresponding reference (seeding) BOLD time courses from a representative rat (Rat 3). It illustrates how the spatiotemporal correlations of spontaneous BOLD signals and associated resting-state coherent networks change under various anesthesia conditions. Under the deep anesthesia with 1.8 % isoflurane, spontaneous BOLD signals had strong temporal correlations over most cortical and some sub-cortical regions covered by the rs-fMRI slices; and the spatial pattern of the correlation maps was insensitive to the location of the reference regions (see the upper part of the right panel in Fig. 1a). This observation suggests that a highly coherent but spatially less-specific network covering a wide range of brain regions exists in the deeply anesthetized rat brain. Strong BOLD correlations under this condition are clearly evident in the BOLD time courses extracted from the selected reference regions, i.e., the left and right S1FL, and the right S1BF regions (Fig. 1a, the lower part of the right panel). These BOLD time courses display large, spontaneous triangular-shaped bumps, which are highly synchronized over the three reference brain regions.

In contrast, the patterns of both correlation maps and BOLD time courses differ substantially under the light anesthesia condition with 1 % isoflurane. The BOLD time courses from the reference regions had distinct fluctuation patterns; the stereotypic BOLD bumps disappeared even though the BOLD fluctuation magnitude was still considerably large (Fig. 1a, the lower part of the left panel). The temporal correlations between the BOLD time courses under the light anesthesia are not easily judged visually, but could be examined through the correlation maps (Fig. 1a, the upper part of the left panel). The correlation maps with respect to the left and right S1FL reference regions overlap each other and cover very similar brain regions, i.e., the bilateral S1FL brain regions, while the correlation map with respect to the right S1BF region mainly covers the bilateral S1BF regions. These observations suggest that the large, less-specific coherent network observed under the deep anesthesia condition with 1.8 % isoflurane has been reorganized under the light anesthesia with 1.0 % isoflurane into multiple smaller but more spatially specific networks. The correlation pattern and dependence on anesthesia level were consistently observed in other seven individual rats of Group I.

In terms of the specificity of BOLD correlation maps, the moderate anesthesia condition with 1.5 % isoflurane sat between the light and deep anesthesia conditions (Fig. 1a, the upper part of the middle panel); however, the magnitude of spontaneous BOLD fluctuations (Fig. 1a, the lower part of the middle panel) was the smallest among the three anesthesia conditions.

To further quantify the BOLD fluctuation pattern changes under different anesthesia conditions, the power spectra of the BOLD time courses were estimated, averaged over all rats, and are shown in Fig. 1b. The substantial change in BOLD fluctuation patterns leads to distinct spectra under different anesthesia conditions. The BOLD spectrum for the light anesthesia has relatively higher power on all frequency ranges compared to the other two conditions. The spectra for the moderate and deep anesthesia cross each other around 0.1–0.15 Hz with the deep anesthesia having higher power in the lower frequency range, which is consistent with the BOLD fluctuation pattern shown in Fig. 1a.

A representative correlation map based on the BOLD signals acquired after the animal was terminated (with the ventilation still running) is also shown in Fig. 1a (lower panel), and only the reference region itself appeared in the map due to autocorrelation. This comparison result suggests that the physiological noise from periodic respiration had a negligible contribution to the BOLD correlations observed in the live rat brain in the present study.

To better quantify the observations described above, the values of the correlation maps within a ROI covering the left-hemisphere cortical regions were projected (by averaging) along the direction orthogonal to the brain midline, and the profiles from all eight rats were then averaged according to anesthesia levels and the results are shown in Fig. 2. The average profiles show strong but relatively uniform CCs over different cortical regions under the deep anesthesia condition (blue curves in Fig. 2). In contrast, they display well-defined and narrow peaks at the position symmetric to the seeding reference regions (in either S1FL or S1BF) under the light anesthesia (red curves). The average profiles of the moderate anesthesia (green curves) again appear intermediate to the other two anesthesia conditions.

For the correlation maps with respect to the right S1FL reference region, the distribution of correlation coefficients within the ROI was estimated through histograms (Fig. 3) for all rats. Under the deep anesthesia, most of rs-fMRI image pixels had very strong correlations, i.e., high CC values, with the seeding reference regions, and this is reflected by the shape of corresponding histogram (blue color), while the histogram for the light anesthesia condition (red color) was more closer to a normal distribution with a much smaller CC mean. The histogram of the moderate anesthesia condition (green color) sat again between the other two conditions. This observation is consistent across different rats (Fig. 3). These results suggest that the specificity of spatiotemporal correlations of spontaneous BOLD fluctuations can change significantly under various anesthesia levels.

Global and System-Specific BOLD Correlations

Removing global signal fluctuation by linear regression is an approach commonly applied in many human rs-fMRI studies to pre-process data before performing correlation analysis (Fox et al. 2009). This approach was applied in the present study to the same rs-fMRI datasets, in parallel, to examine the impact of global BOLD signal fluctuation on the resting-state correlation maps and spatial patterns.

Figure 4 compares the correlation maps from two representative rats (Rats 1 and 6) under the three anesthesia conditions using the same rs-fMRI data pre-processed with and without the global signal regression (GSR). Generally speaking, the GSR had a subtle influence on the correlation maps under the light anesthesia condition (Fig. 4c), but had a profound effect

on those obtained with deep anesthesia. With the GSR, the strong and widely-distributed BOLD correlation over large cortical regions under deep anesthesia was substantially reduced, and specific network patterns appeared in the correlation maps covering more localized and well-defined brain regions, for example, the bilateral S1FL regions (Fig. 4a, bottom row). A similar but less profound effect was also observed under the moderate anesthesia condition (Fig. 4b).

Interestingly, by gradually raising the CC display threshold for the correlation maps obtained without the GSR, the pattern of the resting-state networks under deep anesthesia (Fig. 4a, top row) became similar to those obtained with the GSR (Fig. 4a, bottom row). Therefore, the effect of the GSR in the present study is approximately equivalent to removing the CC range accounting for global correlation (for example, CC < 0.6 for the deep anesthesia) and then expanding the remaining CC range. This comparison suggests that the correlation maps (or the coherent networks) under deep anesthesia are "less-specific" but not completely "non-specific", since the brain regions with the most intensive anatomical connections or structural connectivity, such as the bilateral S1FL regions, still hold the strongest BOLD correlations (or functional connectivity). This notion is supported by the result that the correlation profiles under the deep anesthesia (Fig. 2, blue curves) indeed show peaks (though less sharp) spatially symmetric to their contralateral seeding reference regions.

It is notable that a number of image voxels had negative correlation in the correlation maps after the GSR, though their locations were less consistent compared to the voxels showing positive correlation (Fig. 4).

Effect of Anesthesia on EEG Power Correlations

To further understand the neurophysiology basis of the BOLD coherent network and specificity changes mapped by rs-fMRI, a separate EEG experiment was performed on another group of rats. Figure 5a shows typical EEG signal time courses acquired from a representative rat (Rat 12) under the three anesthesia conditions. The EEG signal under the deep anesthesia had a typical burst-suppression EEG pattern, while no obvious suppression periods were observed for either the light or moderate anesthesia condition. Compared to the light anesthesia, the EEG signals under the moderate level periodically and consistently showed a slow depolarizing transition from low to high voltage, but no significant differences were found between their power spectra (Fig. 5b). In contrast, the EEG power spectrum for the deep anesthesia condition had a significant power reduction, especially in the delta (1–4 Hz) and gamma bands (>30 Hz).

The powers of EEG signals (wide band, 0.1–100 Hz) were also extracted and are shown in Fig. 5c with color encoding locations of the electrodes. The band-pass filter (0.003–0.5 Hz) used for the BOLD signals was also applied on the time courses of EEG power. Compared to the moderate anesthesia, EEG power under the light anesthesia had relatively stronger fluctuation, which is consistent with the BOLD fluctuation amplitude changes observed under these two conditions shown in Fig. 1a. Unlike the rs-fMRI observations, the amplitude of EEG power fluctuations under the deep anesthesia was substantially larger than the other two conditions. Nevertheless, the general trends on anesthesia depth are consistent between EEG and BOLD results.

To investigate the spatial specificity of EEG power correlations while minimizing possible confounding effects caused by cross interference between electrodes in close proximity, we only calculated and compared the EEG power correlation between the left- and right-hemisphere S1FL regions, as well as between the left S1FL region and right S1BF region. Because the left and right S1FL regions belong to a functionally more specific sub-network

compared to the right S1BF region according to the results from our fMRI experiments, we can regard their correlation in part as a within-network correlation and the correlation between the left S1FL and right S1BF as an inter-network correlation. The difference between these two correlation values can then be used to quantify the spatial specificity of EEG power correlations. For the typical EEG runs from the representative rat shown in Fig. 5, we first noticed that the EEG power correlation generally decreased as the anesthesia level was reduced. At the same time, the difference between the within-network correlation (left S1FL versus right S1FL) and the inter-network correlation (left S1FL versus right S1BF) decreased as the level of anesthesia depth went up: 0.17, 0.15, and 0.06 for the light, moderate, and deep anesthesia conditions, respectively. Both trends are consistent with the BOLD correlation observed in the rs-fMRI experiments.

To further quantify the above observation, we performed more detailed analysis on EEG data acquired from all rats in Group II. Besides the power of wide-band EEG (0.1–100 Hz), the power of other band-limited EEG signals were also obtained and the similar correlation analysis was performed on EEG band-limited powers (BLPs). The average results from all the rats are summarized in Fig. 6. Generally, the EEG power correlations significantly increased as the anesthesia depth went up from the light to deep anesthesia. Moreover, we also observed a trend that the differences between the within-network correlation (left S1FL versus right S1FL) and the inter-network correlation (left S1FL versus right S1BF) decreased as the anesthesia level increased, suggesting a change in specificity of EEG power correlations that was similar with the observations of BOLD correlation from the fMRI experiments. It is interesting to note that the trend of correlation difference between the two sub-networks was strongest for the wide band EEG power but weakest for alpha band power. All BLPs of EEG had similar trends describe above, but the results from high-frequency beta and gamma bands were more consistent across individuals and also more stable over time in the same animal.

Correlations of EEG signal itself (based on phase coherence) other than the power were also calculated (the results were not shown herein). Compared to the power correlation, the phase correlation did not show consistent trends across individual animals, especially for the high-frequency beta and gamma bands.

Discussion and Conclusion

In this study, the analysis of spatiotemporal correlations of spontaneous BOLD fluctuations in the anesthetized rat brain revealed that the specific resting-state coherent networks covering distinct sub-regions of the rat sensorimotor system gradually merged into a highly-coherent but less-specific network covering almost the entire cortical region when the anesthesia depth changed from light to deep. The corresponding EEG measurements under the same conditions showed that EEG power correlations had similar dependency on anesthesia levels, suggesting the neural origin of the network specificity change observed by rs-fMRI BOLD signals. This finding may suggest a reorganization of ongoing brain activity pattern across different brain states, which can be robustly imaged and studied by rs-MRI.

Spontaneous BOLD Fluctuations Under Various Anesthesia Levels

Spontaneous BOLD signal under the light anesthesia showed specific correlation patterns covering distinct subregions of the rat somatosensory system, e.g., the bilateral S1FL versus S1BF regions. This finding is consistent with the pattern of the resting-state network observed in the lightly anesthetized rats with medetomidine sedation (Zhao et al. 2008). Such somatotopic organization of resting-state functional connectivity is also in agreement with those observed in the primary motor cortex of awake human subjects (van den Heuvel and Hulshoff Pol 2009) and awake rats (Liang et al. 2011). Collectively, these results

suggest that the network specificity may be one of important characteristics of the resting-state functional connectivity under awake and lightly anesthetized brain states. The specific networks mapped by rs-fMRI may reflect the underlying neuroanatomical connectivity associated with their brain functionalities.

Compared to the light anesthesia, spontaneous BOLD signals measured under the deep anesthesia condition showed a completely different temporal fluctuation pattern: the large, stereotypic triangular-shaped BOLD bumps appeared intermittently and spontaneously. The synchronization of these bumps leads to strong and widely distributed correlation of BOLD signals over large cortical regions much beyond the sensorimotor system. It has been shown previously (Liu et al. 2011) that such a unique pattern was induced by the BS EEG pattern under the deep isoflurane anesthesia (1.8 %), which consists of alternating spontaneous high-voltage EEG bursts and suppressed near-flat EEG periods (Kroeger and Amzica 2007; Stern and Engel 2005). Therefore, the spontaneous BOLD signals under the deep anesthesia condition still reflect the ongoing brain activity fluctuation, and their temporal correlations reveal the connectivity between different brain regions under this unconscious condition.

As the transition stage, the moderate anesthesia condition with 1.5 % isoflurane shows the smallest magnitude of spontaneous BOLD fluctuations (Fig. 1a). In rats, isoflurane can induce the BS EEG pattern at concentrations of 1.4–1.8 % (Hudetz and Imas 2007), and the appearance frequency of spontaneous EEG bursts is known to decrease as isoflurane concentration increases within this range. At the moderate anesthesia level (~1.5 % isoflurane), the EEG bursts probably occur so frequently as to result in substantial overlapping between adjacent BOLD bumps; therefore, a relatively "flat" BOLD time course without obvious bumps was observed (e.g., Fig. 1a, the lower part of the middle panel). Interestingly, even though the BOLD time courses were relatively flat, their temporal correlations were still strong and followed an expected transition trend between the light and deep anesthesia levels. This finding is supported by distinct EEG and power patterns observed under the moderate and deep anesthesia conditions as discussed below.

A number of studies have examined how anesthesia or sedation affects the resting-state functional connectivity with different findings. Some of them reported a decrease of functional connectivity as anesthesia level increases (Peltier et al. 2005; Martuzzi et al. 2010; Liu et al. 2011; Wang et al. 2011), while others showed opposite results (Kiviniemi et al. 2000, 2005), or negligible effect of anesthesia depth on resting-state networks (Vincent et al. 2007). These discrepancies could be explained by many reasons, including the differences in species studied, the types and dosages of anesthetic agents used, or the resting-state networks investigated. However, different strategies used for rs-fMRI data analysis, for example, whether or not to remove global signal fluctuation, could also lead to different outcomes.

Pattern and Correlation Changes of EEG Under Various Anesthesia Levels

The power of EEG signals, acquired from the second group of rats, show distinct patterns that accord well with the spontaneous BOLD signal fluctuation patterns under corresponding anesthesia conditions, except that the EEG power shows much stronger fluctuation under the deep anesthesia than under the other two conditions while the BOLD signal fluctuation does not. This is difficult to explain at the current stage without knowing the exact relationship between hemodynamic signal and electrophysiology signal, for example, how band-limited EEG signals at different frequency ranges contribute to the BOLD signal.

The EEG power correlation also showed similar dependency on anesthesia as the spontaneous BOLD correlation. For both modalities, the general correlation strength increased under deeper anesthesia, while the dominance of within-network correlation to

inter-network correlation, i.e., spatial specificity, decreased as the anesthesia level increased. Although certain frequency bands, e.g., beta and gamma bands show less inter-subject variation than others, e.g., alpha band, all BLPs of EEG basically gave similar results. However, neither of these trends could be observed when the correlation analysis was applied to EEG signal (or band-limited signal) itself instead of its powers.

In general, the analogy between BOLD and EEG power correlations supports previous finding of a close coupling between spontaneous BOLD signal and underlying EEG (or local field potential) power (Feige et al. 2005; Lu et al. 2007; Nir et al. 2008; Shmuel and Leopold 2008) and also suggests that the specificity change of functional connectivity originates from the modulation of underlying neural activity and its synchrony.

For both BOLD and EEG experiments, the correlation pattern under the moderate anesthesia is more similar to the light anesthesia than to the deep anesthesia, suggesting that such a specific-to-less-specific transition may not be a linear function of the isoflurane concentration. When comparing the specificity of EEG power correlation (i.e., the difference between the within- and inter-network correlation) under the light and moderate conditions, the statistical significance was only found for the wide-band EEG power even though all EEG BLPs showed consistently higher specificity under the light anesthesia. This may attribute to the reduced statistical power caused by large inter-subject variation in EEG power correlation, which, in turn, may result from many factors, e.g., the different tolerance level to anesthetic agent.

Functional Connectivity Specificity and Global Signal Regression

GSR is a common practice in rs-fMRI studies, in particular for human application (Fox et al. 2009). One merit of this approach is to remove, or at least reduce, globally correlated noise introduced by instability of data acquisition, head motion or non-neural physiological sources (e.g., respiration and heart pulsation). Since the main goal of most rs-fMRI studies is to identify the correlation patterns of spontaneous BOLD fluctuations specific to the resting-state brain networks of interest, the removal of the global signal fluctuations from either non-neural or less localized neural origins should help to achieve this goal by largely enhancing the rs-fMRI specificity for identifying resting-state networks, for instance, the default mode network (Fox et al. 2009).

The present study did not draw its conclusions merely based on the results using the GSR for the following two reasons. First, the large, global BOLD fluctuation observed under the deep anesthesia with the BS EEG pattern has been shown to originate from the underlying spontaneous neuronal activity (Liu et al. 2011); it therefore may contain vital information regarding spontaneous brain activity. Such a tight neuro-BOLD coupling is also supported by the completely diminished BOLD correlations in the absence of EEG activity after the animal was terminated (see an example shown in Fig. 1a), suggesting that the global, non-neural signal had a negligible effect on the correlation analysis in the present study. Moreover, a recent study has also shown a widely distributed brain activity fluctuation in the primate and its correlation with spontaneous BOLD signals (Scholvinck et al. 2010). Together, these findings underscore the essential contribution from the globally coherent neuronal activity on the resting-state functional connectivity. Second, the main focus of the present study is to understand the overall impact of anesthesia level on the "specificity" of resting-state networks, and this goal cannot be achieved if the GSR was applied to remove the global, less-specific BOLD correlation component and thus increase the specificity of resting-state networks under all the anesthesia conditions to a very similar level (see Fig. 4). Therefore, extra caution should be taken when applying the GSR approach, since it will remove the global correlation component that may be more sensitive to the change of brain states, as shown in the present study.

Quantification of Functional Connectivity Specificity

It is clear that not only the temporal correlation strength (CC value) but also the spatial specificity is essential for the interpretation and understanding of resting-state networks and their impact on brain functions. One relevant question is therefore how to quantify the specificity of resting-state coherent network using rs-fMRI.

We have found that even under deep anesthesia the widely distributed network is "less-specific", but not completely "non-specific". The bilateral homologous brain regions (e.g., bilateral S1FL or S1BF regions studied herein) still have the strongest BOLD coherence, which are clearly evident on the CC profiles (Fig. 2) and the correlation maps derived with the GSR (Fig. 4). Therefore, the term "specificity" is a relative rather than absolute concept, and it refers to the relative contributions between the BOLD correlation specific to functional networks and the global, less-specific BOLD correlation, which may reflect independent neuronal processes.

The present study has shown that the GSR is an effective method to separate these two correlation components by removing the global BOLD correlation component (Fig. 4). Therefore, a simple rs-fMRI approach for quantifying the specificity of brain networks is to compare the difference of correlation strength within a network of interest before and after the use of the GSR, and this can estimate how much the global, non-specific BOLD correlation accounts for the total BOLD correlation within the same network, thus, provide a qualitative measure of network specificity. For instance, the GSR resulted in a much larger reduction in BOLD correlations of the rat sensorimotor network under deep than light anesthesia condition as demonstrated in Fig. 4, indicating a less specific network under deep anesthesia. However, one should be cautious about this approach if the global BOLD correlation is dominated by non-neural physiological noise rather than ongoing neural activity. Another drawback of this approach is that the GSR might be prone to induce spurious negative correlations (Murphy et al. 2009). For these considerations, more sophisticated algorithms able to correct physiological noise without affecting neural signals are desirable. A recent study has shown that the global component can be quantified using the principal component (PC) that correlates better with the average global signal. Therefore, the corresponding eigenvalue for this PC could be a good choice for quantifying the strength of the global component and for performing the global signal regression in an artifact-free manner (Carbonell et al. 2011).

Specificity Change: Unbalanced Integration and Segregation?

According to a new theory about consciousness and anesthesia (Alkire et al. 2008; Hudetz 2006), there are two possible working mechanisms about how anesthesia affects brain function and consciousness. One is to break down cortical connectivity and thus the brain's ability of integration (the loss of integration); and the other is to disrupt the repertoire of cortical activity pattern and thus the brain's capacity for encoding information, even though information may still be integrated globally (the loss of segregation). Essential evidence for supporting the second mechanism comes from rat studies. In deeply anesthetized rats with 1.8 % isoflurane showing BS EEG activity (the same model used in the present study), visual stimulation evoked global and highly synchronized field potential responses in many brain regions including the occipital, parietal, and frontal lobes that are much beyond the visual system, indicating a loss of function specificity; in contrast, the same stimulation on awake rat brain elicited neuronal responses confined only within the visual cortex (Hudetz and Imas 2007). The findings of the present study support the second mechanism from a unique neuroimaging perspective. Under the completely unconscious state induced by deep anesthesia, not only did BOLD signals show a stereotypic fluctuation pattern, but the multiple discriminable resting-state networks (implied by BOLD correlations) as observed

under the light anesthesia merged into one widely-distributed and less-specific network with stronger BOLD correlation. Our study provides evidence that the repertoire of cortical activity pattern (the multiple specific resting-state coherent networks) collapses even though the global integration still remains.

The relationship between increased neuronal synchrony and deepened anesthesia level has been observed in cats anesthetized with agents other than isoflurane. It has been found from an electrophysiology study that under the anesthesia condition showing sleep-like slow wave EEG patterns, additional doses of urethane, ketamine-xylazine, or N_2O could largely increase temporal correlations between cortical and thalamocortical neurons (Contreras and Steriade 1997). Moreover, this highly synchronized activity transcends the borders limiting the functioning of the waking brain, and unites neurons located distantly and belonging to different brain systems into large neuronal assemblies. Therefore, the network specificity change may not be unique only to anesthesia induced by isoflurane.

On the other hand, the dependence of network specificity on the anesthesia level as observed in the present study may not be generalized to any anesthesia conditions. The spatial specificity of functional connectivity in the rats with deep anesthesia induced by alpha-chloralose has showed opposite dependency on the level of anesthesia: the high dose alpha-chloralose was found to significantly reduce the long-range inter-hemispheric BOLD correlation between bilateral S1FL regions (Lu et al. 2007). Moreover, even with isoflurane, the specificity change of functional connectivity is not a monotonic function of anesthesia level. The strength and specificity of functional connectivity in the rat brain could be reduced if the dosage of isoflurane is increased to an even higher level (e.g., 2.2 %) than the deep anesthesia condition with 1.8 % used in this study (Liu et al. 2011) owing to severe suppression of spontaneous EEG activity under very deep anesthesia condition, and they could eventually approach to zero after the animals were terminated.

Specificity Change: Unbalanced Excitation and Inhibition?

In parallel to integration and segregation concepts from a perspective of information processing, the change of functional connectivity specificity may also be explained in the frame of the brain's excitation and inhibition. The spatial specificity may possibly be linked to the rivalry of these two types of brain activities, because the brain's long-range connections are mainly accomplished by excitatory pyramidal neurons, while the inhibitory inter-neurons mainly show local and short connections.

As discussed in the last section, the rat brain characterized with the BS EEG pattern under the deep anesthesia condition is in a "hyper-excitable" state, during which different types of stimulation (e.g., visual, auditory, and somatosensory) can elicit global neuronal responses across different sensory modalities. It has been reported that under the isoflurane-induced BS condition, while the excitatory activity decreased by ~44 %, the inhibitory activity had a more dramatic reduction to approaching almost zero (Ferron et al. 2009). These unmatched changes resulted in a new balance between excitation and inhibition, which could be responsible for the hyper-excitability, and the less-specific functional connectivity of the brain under the BS condition.

It is also interesting to note that alpha-chloralose induces anesthesia effects through a completely different mechanism: it enhances the activity of gamma-aminobutyric acid type A (GABAA) receptors and thus the inhibitory activity of GABAergic interneurons, and could shift the balance of excitation and inhibition towards an opposite direction (Garrett and Gan 1998). Accordingly, the alpha-chloralose showed completely opposite effect on the spatial specificity of functional connectivity (Lu et al. 2007) compared to isoflurane. Collectively, these studies suggest a potential link between the spatial specificity of

functional connectivity and the balance between neuronal excitation and inhibition. More systemic and well-designed studies are needed to better understand the link, and rs-fMRI should play a critical role for the studies.

Acknowledgments

References

Alkire MT, Hudetz AG, Tononi G. Consciousness and anesthesia. Science. 2008; 322(5903):876–880. [PubMed: 18988836]

Bates D, Maechler M, Bloker B. lme4: linear mixed-effects models using S4 classes. R package version. 2011 0999375-39.

Biswal B, Yetkin FZ, Haughton VM, Hyde JS. Functional connectivity in the motor cortex of resting human brain using echo-planar MRI. Magn Reson Med. 1995; 34(4):537–541. [PubMed: 8524021]

Boly M, Tshibanda L, Vanhaudenhuyse A, Noirhomme Q, Schnakers C, Ledoux D, Boveroux P, Garweg C, Lambermont B, Phillips C, Luxen A, Moonen G, Bassetti C, Maquet P, Laureys S. Functional connectivity in the default network during resting state is preserved in a vegetative but not in a brain dead patient. Hum Brain Mapp. 2009; 30(8):2393–2400. [PubMed: 19350563]

Carbonell F, Bellec P, Shmuel A. Global and system-specific resting-state FMRI fluctuations are uncorrelated: principal component analysis reveals anti-correlated networks. Brain Connect. 2011; 1(6):496–510. [PubMed: 22444074]

Contreras D, Steriade M. State-dependent fluctuations of low-frequency rhythms in corticothalamic networks. Neuroscience. 1997; 76(1):25–38. [PubMed: 8971756]

Cox RW. AFNI: software for analysis and visualization of functional magnetic resonance neuroimages. Comput Biomed Res. 1996; 29(3):162–173. [PubMed: 8812068]

Du F, Zhu XH, Zhang Y, Friedman M, Zhang N, Ugurbil K, Chen W. Tightly coupled brain activity and cerebral ATP metabolic rate. Proc Natl Acad Sci USA. 2008; 105(17):6409–6414. [PubMed: 18443293]

Feige B, Scheffler K, Esposito F, Di Salle F, Hennig J, Seifritz E. Cortical and subcortical correlates of electroencephalo-graphic alpha rhythm modulation. J Neurophysiol. 2005; 93(5):2864–2872. [PubMed: 15601739]

Ferron JF, Kroeger D, Chever O, Amzica F. Cortical inhibition during burst suppression induced with isoflurane anesthesia. J Neurosci Off J Soc Neurosci. 2009; 29(31):9850–9860.

Fox MD, Raichle ME. Spontaneous fluctuations in brain activity observed with functional magnetic resonance imaging. Nat Rev Neurosci. 2007; 8(9):700–711. [PubMed: 17704812]

Fox MD, Zhang D, Snyder AZ, Raichle ME. The global signal and observed anticorrelated resting state brain networks. J Neurophysiol. 2009; 101(6):3270–3283. [PubMed: 19339462]

Garrett KM, Gan J. Enhancement of gamma-aminobutyric acidA receptor activity by alpha-chloralose. J Pharmacol Exp Ther. 1998; 285(2):680–686. [PubMed: 9580613]

Greicius MD, Kiviniemi V, Tervonen O, Vainionpaa V, Alahuhta S, Reiss AL, Menon V. Persistent default-mode network connectivity during light sedation. Hum Brain Mapp. 2008; 29(7):839–847. [PubMed: 18219620]

Horovitz SG, Fukunaga M, de Zwart JA, van Gelderen P, Fulton SC, Balkin TJ, Duyn JH. Low frequency BOLD fluctuations during resting wakefulness and light sleep: a simultaneous EEG-fMRI study. Hum Brain Mapp. 2008; 29(6):671–682. [PubMed: 17598166]

Hudetz AG. Suppressing consciousness: mechanisms of general anesthesia. Seminars Anesth Periop Med Pain. 2006; 25:196–204.

Hudetz AG, Imas OA. Burst activation of the cerebral cortex by flash stimuli during isoflurane anesthesia in rats. Anesthesiology. 2007; 107(6):983–991. [PubMed: 18043067]

Kiviniemi V, Jauhiainen J, Tervonen O, Paakko E, Oikarinen J, Vainionpaa V, Rantala H, Biswal B. Slow vasomotor fluctuation in fMRI of anesthetized child brain. Magn Reson Med. 2000; 44(3): 373–378. [PubMed: 10975887]

Kiviniemi VJ, Haanpaa H, Kantola JH, Jauhiainen J, Vainionpaa V, Alahuhta S, Tervonen O. Midazolam sedation increases fluctuation and synchrony of the resting brain BOLD signal. Magn Reson Imaging. 2005; 23(4):531–537. [PubMed: 15919598]

Kroeger D, Amzica F. Hypersensitivity of the anesthesia-induced comatose brain. J Neurosci. 2007; 27(39):10597–10607. [PubMed: 17898231]

Liang Z, King J, Zhang N. Uncovering intrinsic connectional architecture of functional networks in awake rat brain. J Neurosci. 2011; 31(10):3776–3783. [PubMed: 21389232]

Liu X, Zhu XH, Zhang Y, Chen W. Neural origin of spontaneous hemodynamic fluctuations in rats under burst-suppression anesthesia condition. Cereb Cortex. 2011; 21(2):374–384. [PubMed: 20530220]

Lu H, Zuo Y, Gu H, Waltz JA, Zhan W, Scholl CA, Rea W, Yang Y, Stein EA. Synchronized delta oscillations correlate with the resting-state functional MRI signal. Proc Natl Acad Sci USA. 2007; 104(46):18265–18269. [PubMed: 17991778]

Mantini D, Perrucci MG, Del Gratta C, Romani GL, Corbetta M. Electrophysiological signatures of resting state networks in the human brain. Proc Natl Acad Sci USA. 2007; 104(32):13170–13175. [PubMed: 17670949]

Martuzzi R, Ramani R, Qiu M, Rajeevan N, Constable RT. Functional connectivity and alterations in baseline brain state in humans. Neuroimage. 2010; 49(1):823–834. [PubMed: 19631277]

Murphy K, Birn RM, Handwerker DA, Jones TB, Bandettini PA. The impact of global signal regression on resting state correlations: are anti-correlated networks introduced? Neuroimage. 2009; 44(3):893–905. [PubMed: 18976716]

Nir Y, Mukamel R, Dinstein I, Privman E, Harel M, Fisch L, Gelbard-Sagiv H, Kipervasser S, Andelman F, Neufeld MY, Kramer U, Arieli A, Fried I, Malach R. Interhemispheric correlations of slow spontaneous neuronal fluctuations revealed in human sensory cortex. Nat Neurosci. 2008; 11(9):1100–1108. [PubMed: 19160509]

Paxinos, G.; Watson, C. The rat brain in stereotaxic coordinates. San Diego: Academic Press; 1998.

Peltier SJ, Kerssens C, Hamann SB, Sebel PS, Byas-Smith M, Hu X. Functional connectivity changes with concentration of sevoflurane anesthesia. NeuroReport. 2005; 16(3):285–288. [PubMed: 15706237]

Raichle ME. Neuroscience. The brain's dark energy. Science. 2006; 314(5803):1249–1250. [PubMed: 17124311]

Scholvinck ML, Maier A, Ye FQ, Duyn JH, Leopold DA. Neural basis of global resting-state fMRI activity. Proc Natl Acad Sci USA. 2010; 107(22):10238–10243. [PubMed: 20439733]

Shmuel A, Leopold DA. Neuronal correlates of spontaneous fluctuations in fMRI signals in monkey visual cortex: implications for functional connectivity at rest. Hum Brain Mapp. 2008; 29(7):751–761. [PubMed: 18465799]

Shulman RG, Rothman DL, Hyder F. A BOLD search for baseline. Neuroimage. 2007; 36(2):277–281. [PubMed: 17223362]

Stern, JM.; Engel, J. Atlas of EEG patterns. Philadelphia: Lippincott Williams & Wilkins; 2005. p. 107-108.

Team, RDC. R: A language and environment for statistical computing. Vienna: R Foundation for Statistical Computing; 2008.

Thomson DJ. Spectrum estimation and harmonic analysis. Proc IEEE. 1982; 70:1055–1096.

van den Heuvel MP, Hulshoff Pol HE. Specific somatotopic organization of functional connections of the primary motor network during resting state. Hum Brain Mapp. 2009; 31(4):631–644. [PubMed: 19830684]

Vincent JL, Patel GH, Fox MD, Snyder AZ, Baker JT, Van Essen DC, Zempel JM, Snyder LH, Corbetta M, Raichle ME. Intrinsic functional architecture in the anaesthetized monkey brain. Nature. 2007; 447(7140):83–86. [PubMed: 17476267]

Wang K, van Meer MP, van der Marel K, van der Toorn A, Xu L, Liu Y, Viergever MA, Jiang T, Dijkhuizen RM. Temporal scaling properties and spatial synchronization of spontaneous blood

oxygenation level-dependent (BOLD) signal fluctuations in rat sensorimotor network at different levels of isoflurane anesthesia. NMR Biomed. 2011; 24(1):61–67. [PubMed: 20669170]

Williams KA, Magnuson M, Majeed W, LaConte SM, Peltier SJ, Hu X, Keilholz SD. Comparison of alpha-chloralose, medetomidine and isoflurane anesthesia for functional connectivity mapping in the rat. Magn Reson Imaging. 2010; 28(7):995–1003. [PubMed: 20456892]

Zhang D, Raichle ME. Disease and the brain's dark energy. Nat Rev Neurol. 2010; 6(1):15–28. [PubMed: 20057496]

Zhao F, Zhao T, Zhou L, Wu Q, Hu X. BOLD study of stimulation-induced neural activity and resting-state connectivity in medetomidine-sedated rat. Neuroimage. 2008; 39(1):248–260. [PubMed: 17904868]
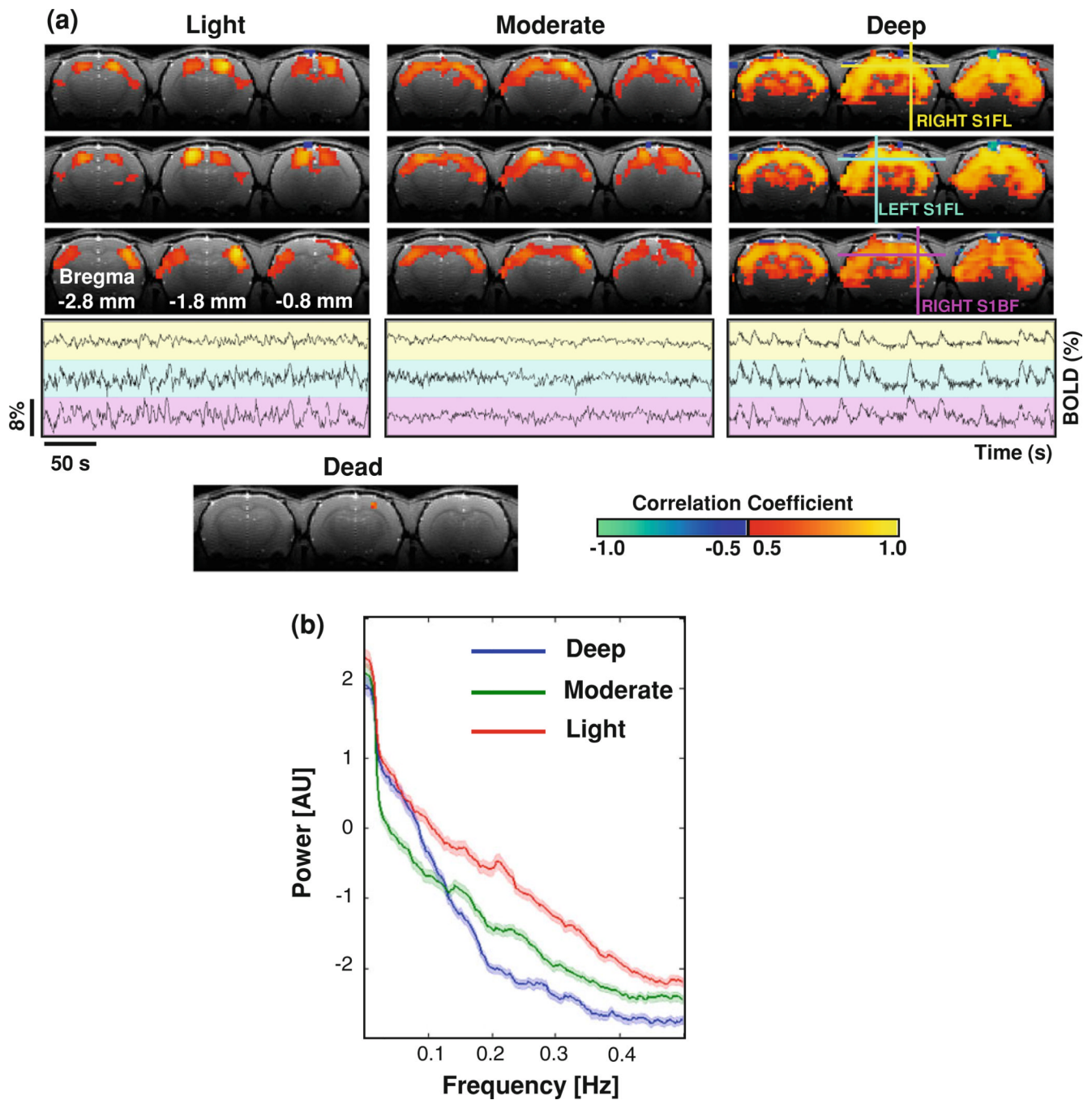
Fig. 1.
a BOLD correlation maps and corresponding reference time courses from a representative rat. Top three rows display BOLD correlation maps with respect to the bilateral S1FL (*yellow* and *blue* cross) and the right S1BF (*magenta* cross) regions, respectively, under the light (*left panel*), moderate (*middle panel*), and deep (*right panel*) anesthesia conditions; and the BOLD time courses from these reference regions are plotted on a background with corresponding color at the bottom row. The BOLD signals demonstrate distinct fluctuation patterns at different anesthesia level, and the specificity of their correlation maps decreases as the anesthesia increase from light to deep. A correlation map with respect to the right

S1FL obtained after the rat being terminated (*lower left panel*) only shows the reference region, indicating a diminished BOLD correlation at this condition. **b** Power spectra of BOLD signals. The power spectra (0–0.5 Hz) of spontaneous BOLD signals at the three seeding locations were estimated for the light (*red line*, n = 84, three spectra for each rs-fMRI run), moderate (*green line*, n = 78) and deep (*blue line*, n = 93) anesthesia conditions and summarized from all the rats with fMRI measurement. Shadows regions are within two standard errors
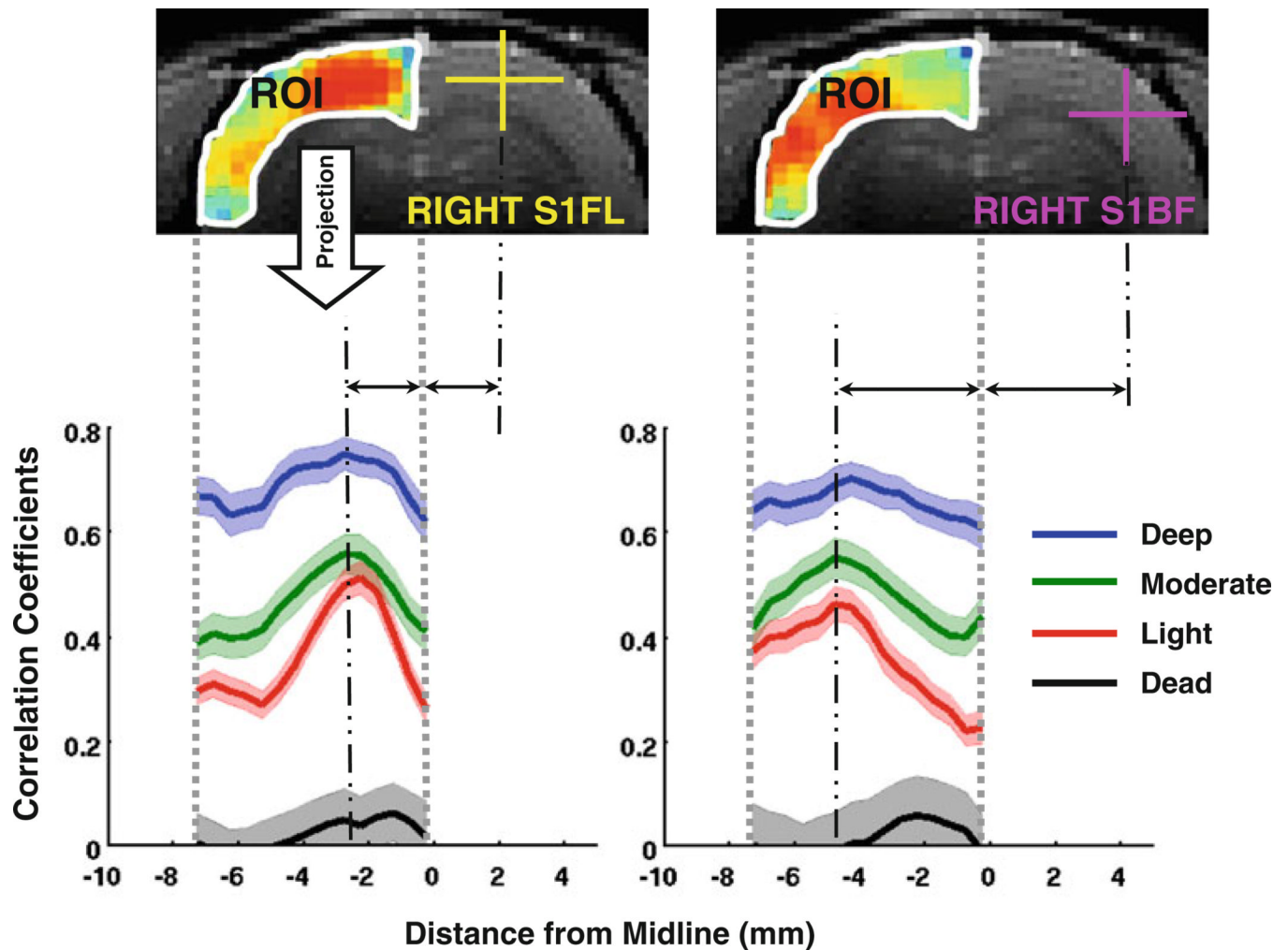
Fig. 2.
Projection of BOLD correlation maps (using the rs-fMRI data of light anesthesia for demonstration) onto a line orthogonal to the brain midline. Within a ROI covering the left-hemisphere cortical regions, the BOLD correlation maps with respect to the S1FL (*left*) and S1BF (*right*) regions from all the rats (n = 8) was projected onto a line orthogonal to the brain midline by averaging in vertical. The projection profiles show distinct, sharp peaks at the locations symmetric to the reference regions under the light anesthesia (*red*, n = 28 runs), but are relatively uniform at the deep anesthesia (*blue*, n = 31 runs), with the profiles for the moderate anesthesia (*green*, n = 26 runs) sitting between them. After the animals were terminated, the profiles (*black*, n = 16 runs) approach the zero line. Shadowed regions are within two standard errors
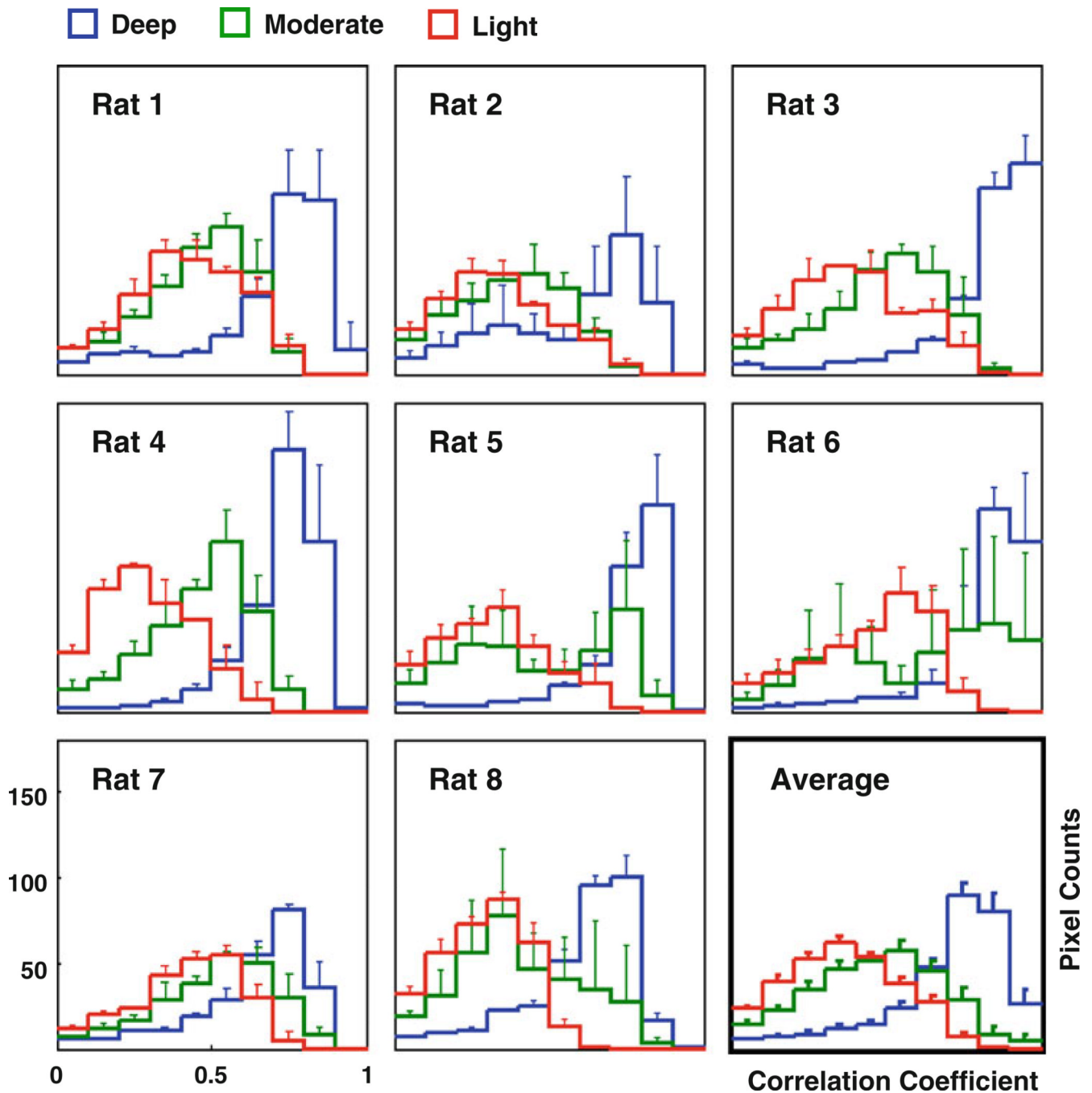
Fig. 3.
Histograms showing the positive CC distribution of correlation maps with a ROI covering the left-hemisphere cortical regions (see Fig. 2). The distribution of CC values under the deep anesthesia (*blue*) is consistent with the strong, but less-specific correlation pattern. In contrast, the CC distribution at the light anesthesia (*red*) is closer to a normal distribution, and that under the moderate anesthesia (*green*) sits between those of the other two conditions. The above observation is consistent across individuals. Only a few pixels showed negative CC values in the correlation maps and are therefore not shown in the histograms. The *error bars* stand for the standard errors across runs
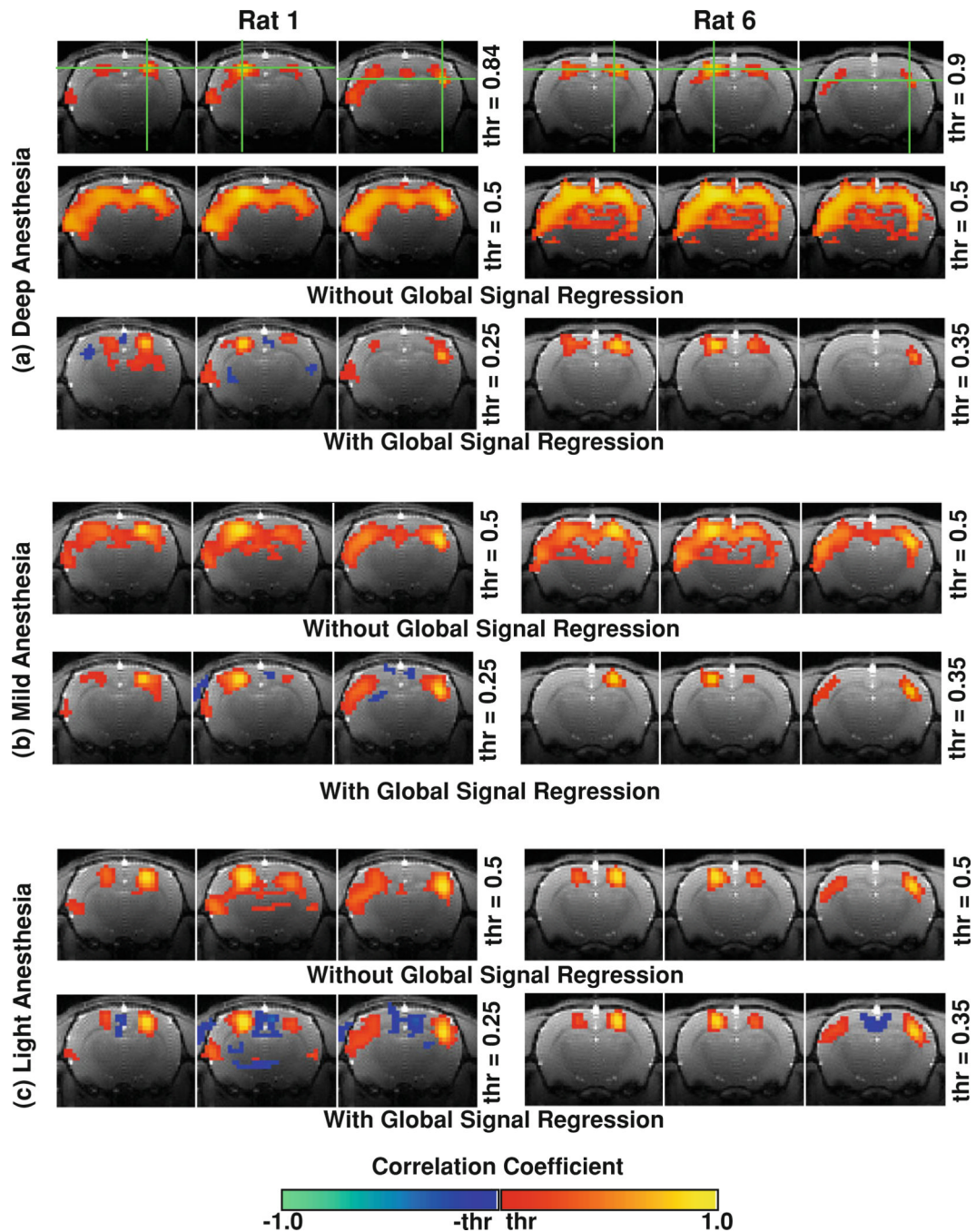
Fig. 4.
Correlation maps from two representative rats generated with and without global signal regression. The correlation maps under the deep anesthesia (the second row of **a**) became much more specific after the global BOLD fluctuation was removed by regression (the bottom row of **a**). Such specific patterns, however, can also be obtained by adjusting the CC threshold (thr) to a much higher value (the top row of **a**). This finding suggests a "less-specific" but not completely "non-specific" correlation pattern for the spontaneous BOLD signals under the deep anesthesia. The global signal regression has a similar but less

profound effect on the moderate (**b**) and light (**c**) anesthesia conditions compared to the deep (**a**) anesthesia condition
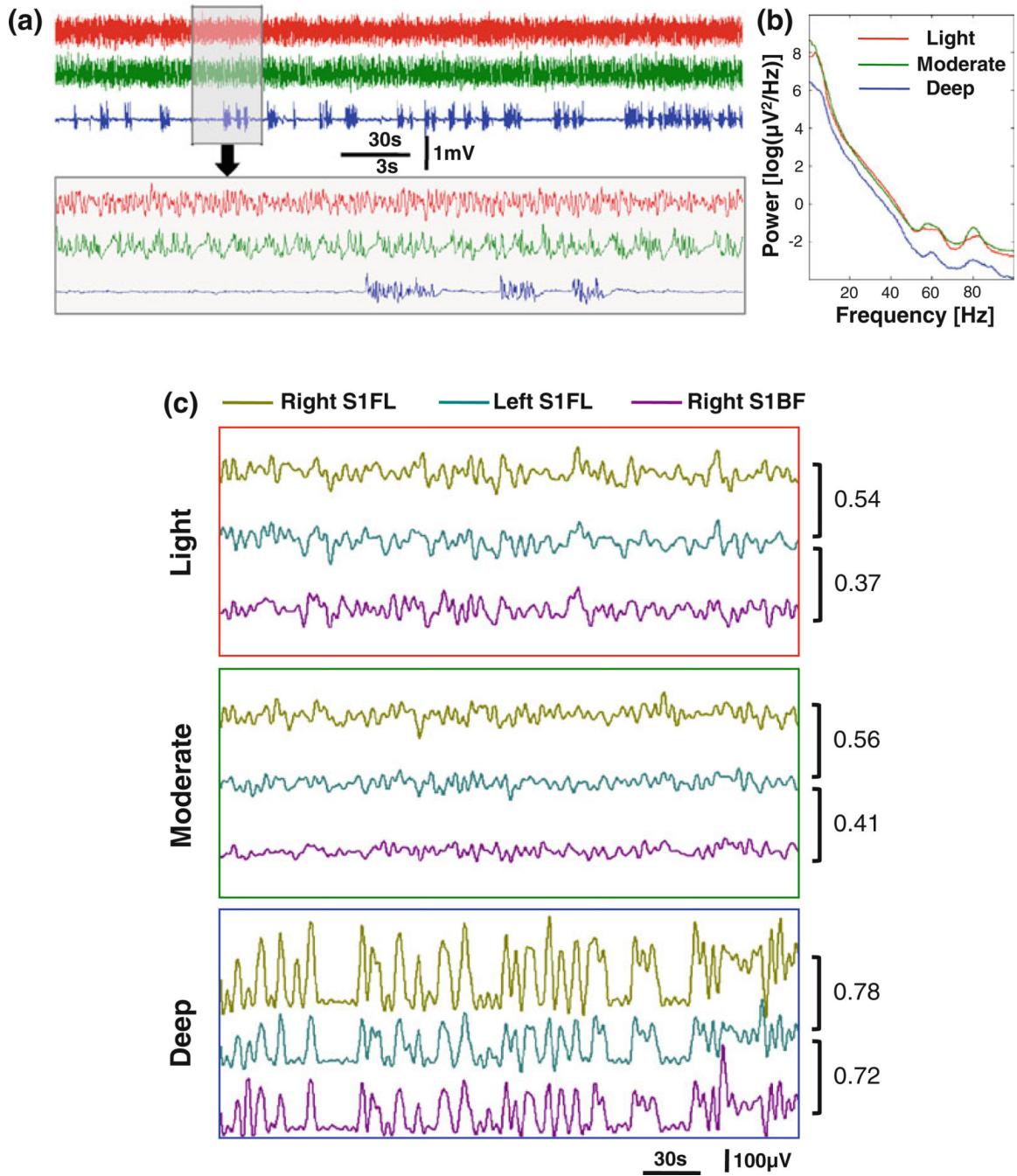
Fig. 5.
EEG signals from a representative rat. Three EEG segments (**a**) recorded under the light (*red*), moderate (*green*), and deep (*blue*) anesthesia conditions respectively and their corresponding power spectra (**b**) demonstrate distinct patterns. The power (amplitude envelope) of EEG signals (**c**) shows slow, spontaneous fluctuation, which also has distinct patterns at different anesthesia levels. The EEG power correlations between different brain regions indicate an increased synchronization and a reduced specificity (see discussion in "Results" section) under the deeper anesthesia condition. *Note* the numbers in (**c**) are correlation coefficients between corresponding EEG power time courses
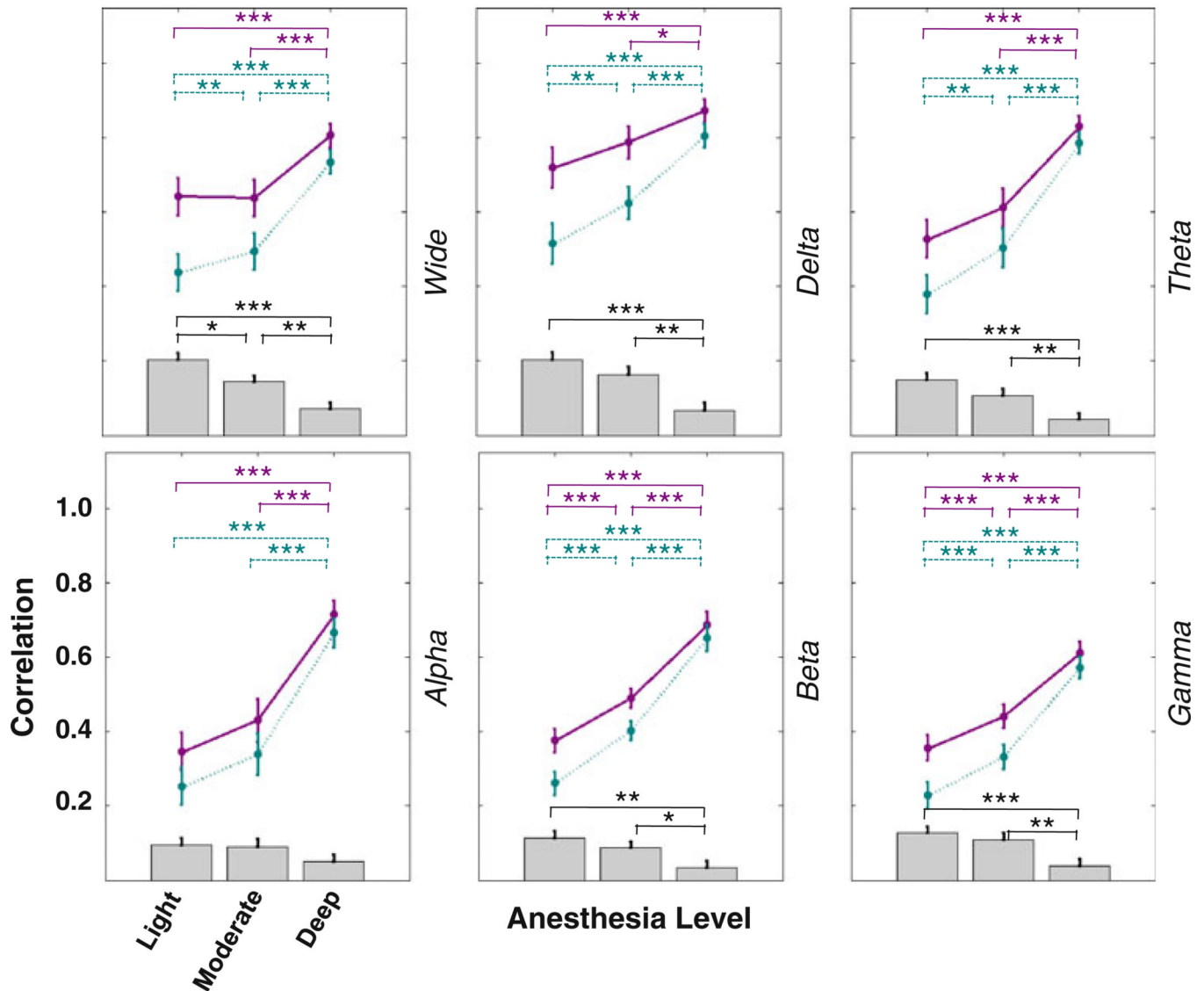
Fig. 6.
EEG power correlation results summarized from all rats with EEG recording (n = 6). The power (amplitude envelope) of the wide band (*top left*), delta band (*top middle*), theta band (*top right*), alpha band (*bottom left*), beta band (*bottom middle*), and gamma band (*bottom right*) were extracted, and their correlations were calculated between the left and right S1FL regions (regarded as the within-network correlation, *dark magenta*) and between the left S1FL and right S1BF regions (regarded as the inter-network correlation, *dark cyan*) and are displayed as scatter plots. Their correlation differences are also displayed as the column plot (*gray color*) beneath the *scatter plots*. *Error bars* stand for standard errors (n = 6) and *star* symbols indicate statistical significance level (*$p<0.05$; **$p<0.01$; and ***$p<0.001$)

Table 1

Mean arterial pressure and heart rate under varied anesthesia levels (n = 14)

Anesthesia condition (% Isoflurane)	Mean arterial pressure (Mean ± SD)	Heart rate (Mean ± SD)
Light (1.0 %)	113.4 ± 11.3	404 ± 37
Mild (1.5 %)	106.4 ± 10.8	393 ± 34
Deep (1.8 %)	99.1 ± 10.0	365 ± 22